Electron–molecular vibration coupling in trimerized isostructural mixed-stack complexes (EDT-TTF-I2)2TCNQFn (n = 0, 1, 2)

Arkadiusz Frąckowiak, Roman Swietlik, Iwona Olejniczak, Olivier Jeannin, Marc Fourmigué

Electron – molecular vibration coupling in trimerized isostructural mixed-stack complexes (EDT-TTF-I_2)$_2$TCNQF$_n$ (n = 0, 1, 2)

Arkadiusz Frąckowiak[1], Roman Świetlik[1], Iwona Olejniczak[1], Olivier Jeannin[2], Marc Fourmigué[2]

[1] *Institute of Molecular Physics, Polish Academy of Sciences, Mariana Smoluchowskiego 17, 60-179 Poznań, Poland*

[2] Univ Rennes, CNRS, ISCR (*Institut des Sciences Chimiques de Rennes), Campus de Beaulieu, 35042 Rennes, France*

Abstract

Infrared and Raman spectra of three isostructural charge transfer complexes (EDT-TTF-I_2)$_2$TCNQF$_n$ (n = 0, 1, 2) are studied. The planar molecules in these complexes are arranged in one-dimensional stacks formed by donor-acceptor-donor (DAD) centrosymmetric trimeric units with a different degree of charge transfer between D and A. In the IR electronic spectra two bands attributed to D-D and D-A charge transfer transitions are distinguished. In the IR vibrational spectra, numerous bands related to coupling of D and A intramolecular vibrations with electrons, are seen. The electron–molecular vibration coupling is clearly seen for acceptor modes attributed to C≡N, C=C stretching, and C-H bending as well as for C=C stretching donor modes. These modes are investigated as a function of temperature (T = 300–10 K). The temperature effect is especially significant for the n=1 complex which undergoes a neutral-to-ionic phase transition. In our study we show that the electron–molecular vibration coupling has also an influence on Raman spectra.

1. Introduction

In many charge-transfer (CT) complexes formed by planar π-electron donors (D) and acceptors (A), the molecules are arranged in quasi-one-dimensional segregated or mixed stacks with considerable overlap of molecular π-orbitals which is responsible for strong CT interactions. The complexes with segregated stacks often exhibit a high electrical conductivity. On the other hand, the mixed-stack complexes are usually insulators or semiconductors, nevertheless they attract a considerable attention, mainly because of a possibility of neutral-to-ionic (N-I) phase transition induced by temperature and/or pressure [1, 2]. The best-known and mostly studied N-I transition is observed in the 1:1 complex TTF-CA (TTF = tetrathiafulvalene, CA=chloranil). On temperature decreasing at T=81 K in the TTF-CA crystal the degree of CT (ρ) abruptly changes and the crystal undergoes a transition from formally neutral phase (ρ = 0.3e) to formally ionic phase (ρ = 0.6e) and regular …DADADA… stacks become dimerized [1, 3]. The N-I transition depends on the relative electron affinity of acceptor and ionization potential of donor, inter-molecular hopping integral, electrostatic interaction, interaction of electrons with intramolecular and lattice vibrations. Another interesting mixed stack structure

…DAADDAADD… was found in the CT complex TTF-TCNE (TCNE = tetracyanoethylene) [4], however without N-I transition. In three isostructural complexes (EDT-TTF-I_2)$_2$TCNQF$_n$ (n = 0, 1, 2) the molecules form trimerized mixed stacks …DADDADDA… (where donor EDT-TTF-I_2 is an iodinated TTF derivative and acceptor TCNQF$_n$ is a fluorinated tetracyano-quinidimethane derivative) [5]. An interesting and unique feature is that for n=0 the complex is essentially neutral, for n=1 the degree of CT changes from about 0.2e to about 0.8e on temperature decreasing (N-I transition at about 100 K), and for n=2 a nearly full charge transfer is observed. Indeed, due to fluorination the acceptor reduction potential increases from 0.14 V for TCNQ [6] to 0.26 V for TCNQF [7], 0.30 V for TCNQF$_2$ [8], and 0.40 V for TCNQF$_4$ [9] (versus SCE). Consequently, the complexes yielded by the fluorinated TCNQF$_n$ usually exhibit a higher degree of charge CT in comparison with analogous TCNQ complexes. The fluorinated TCNQF$_n$ (n = 1, 2, 4) derivatives were often used for synthesis of CT salts with interesting properties [10-16].

A characteristic feature of IR spectra of segregated or mixed stack complexes in the non-neutral state is the presence of strong vibronic features being a consequence of electron – intramolecular vibration (EMV) interactions. In comparison with molecular IR active modes the EMV bands usually exhibit high intensity, shift towards lower frequencies, and significant broadening. The optical properties of these CT systems were intensively studied both experimentally and theoretically. Depending on the structure of segregated one-dimensional stacks, various models of EMV coupling were proposed: for dimerized, trimerized, tetramerized, and regular stacks [17-19]. For the mixed stacks, most of the optical studies were performed for the 1:1 complexes with regular and dimerized …ADADAD… stacks. For example, the EMV coupling in TTF-CA in the quasi-neutral phase with regular stacks (T> 81 K) was analyzed with a trimer model and in the dimerized quasi-ionic phase (T< 81 K) with a dimer model [20, 21]. In the trimer model for regular stacks the DA units and also interactions between them are considered. Subsequently, a model of tetramer cluster was developed for a mixed-stack structure of the type …AADDAADD… and used for interpretation of vibrational and electronic spectra of the charge-transfer complex TTF-TCNE [22, 23]. The three isostructural 2:1 complexes (EDT-TTF-I_2)$_2$TCNQF$_n$ (n = 0, 1, 2), with one-dimensional trimerized stacks …DADDAD… and different degree of CT changing from 0 to 1e provide a unique possibility to study the EMV coupling in the mixed stacks consisting of DAD trimers. The opportunity to study a mechanism of a temperature- and/or pressure-induced N-I phase transition in a 2:1 complex, makes (EDT-TTF-I_2)$_2$TCNQF the most interesting complex of the series.

The compounds (EDT-TTF-I_2)$_2$TCNQF$_n$ (n = 0, 1, 2) crystallize in the triclinic system, space group $P\bar{1}$, with EDT-TTF-I_2 donors (D) in a general position in the unit cell and TCNQF$_n$ (n = 0, 1, 2) acceptors (A) in an inversion center. Note that with TCNQF, the single fluorine atom is disordered with 50:50 occupancy on two inversion-centered positions, the very same positions occupied by one fluorine atom in the (EDT-TTF-I_2)$_2$TCNQF$_2$ complex. This implies that from a local point of view, the two EDT-TTF-I_2 molecules surrounding a TCNQF molecule are not exactly similar (see below). The molecules are arranged in the mixed stacks …DADDAD…along the *(a-b)* direction. The mixed-stacks can be considered as consisting of

centrosymmetric DAD trimers interacting with each other inside the stacks (π-orbital overlap). The parallel stacks form layers which are perpendicular to the *c*-axis and the neighboring layers are linked together by C-I···N≡C halogen bonds (Fig. 1). It is important to note that, in addition to intra-stack and side-by-side inter-stack interactions, significant interactions between neighboring layers due to halogen bonding should also be considered [5].

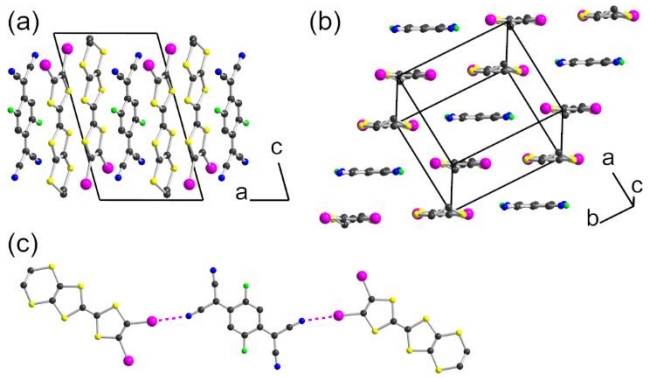

Figure 1. Crystal structure of (EDT-TTF-I_2)$_2$TCNQF$_n$ (n = 0, 1, 2), with (a) projection view along the *b*-axis, (b) view of the DAD alternated stacks running along (*a*-*b*) direction, and (c) detail of the C-I···N≡C halogen bonding interaction, shown by pink dotted lines.

The degree of TCNQ acceptor charge (ρ) in its charge-transfer salts is usually determined from TCNQ bond lengths [24]. Based on the bond lengths from X-ray crystal structure data, it was found that at room temperature (T=293 K) the ρ is 0.2*e*, 0.1*e* and 1.0*e* for (EDT-TTF-I_2)$_2$TCNQ$_n$ (n =0, 1, 2), respectively [5]. At 293 K, the complexes for n=0 (TCNQ) and n=1 (TCNQF) are essentially neutral and the complex for n=2 (TCNQF$_2$) forms an ionic salt (EDT-TTF-$I_2^{+0.5}$)$_2$TCNQF$_2^{-1}$. The low-temperature X-ray structural studies showed that there is no essential modification of ρ in the TCNQ and TCNQF$_2$ compounds down to 20 K. On the other hand, in the TCNQF compound the ρ substantially grows on cooling, what gives evidence of a N-I transition. It is important to emphasize that down to 20 K, all three compounds crystallize in the triclinic crystal structure, without any indication of structural transition, such as the loss of the inversion center at which the acceptors are located [5].

Infrared and Raman spectroscopic studies as a function of temperature gave a convincing evidence of the neutral-to-ionic (N-I) transition in the complex (EDT-TTF-I_2)$_2$TCNQF [5, 25]. It was estimated that the degree of charge transfer (ρ) between donors and acceptor increases from about 0*e* at room temperature to about 1*e* at T= 8 K with a clearly visible regime change at about 100 K. The IR studies of (EDT-TTF-I_2)$_2$TCNQF suggested an existence of considerable EMV coupling for the acceptor C≡N stretching modes. Subsequently, on the basis of the electrical conductivity measurements it was found that hydrostatic pressure can also cause the transition and a pressure-temperature phase diagram was proposed [26]. The N-I transition is a very rear phenomenon and was usually observed in 1:1 organic CT complexes [1]. The observation of temperature induced N-I transition under ambient pressure in the (EDT-TTF-I_2)$_2$TCNQF is the first clear example of such transition in a 2:1 mixed-stack single crystal. In this paper, we want to extend our preliminary investigations of EMV coupling in the TCNQF

complex [5, 25] to the whole series (n = 0, 1, 2), allowing for useful comparison between the three isostructural compounds despite different degrees of charge transfer, highlighting the very important role of partial charge transfer for the observation of strong EMV coupling.

2. Experimental

Single crystals of (EDT-TTF-I_2)$_2$TCNQF$_n$ (n=0, 1, 2) complexes (subsequently labelled as D_2TCNQ, D_2TCNQF, and D_2TCNQF$_2$, respectively) were synthesized and crystallized according to a previously described procedure [5]. Typical dimensions of the elongated plates used in measurements were 0.5 x 0.2 x 0.02 mm^3. The optical axes of the sample were determined as those displaying the largest reflectance anisotropy. The IR spectra were measured in the directions nearly parallel (E$\|$ a-b) and perpendicular (E$\|$ a+b) to the stacking axis. The polarized reflectance (from 600 to 12000 cm^{-1}) and transmittance (from 600 to 4000 cm^{-1}) spectra were recorded with a resolution of 4 cm^{-1} using a Bruker Equinox 55 FT-IR spectrometer equipped with a Hyperion 1000 infrared microscope and a set of suitable polarizers. The absolute values of reflectance were obtained using an aluminum mirror. The optical conductivity was calculated using Kramers-Krönig transformation of the reflectance data [27]. In the low frequency range, the data were extrapolated assuming a constant value appropriate for insulators and in the high frequency range the data were extrapolated assuming a ω^{-2} behavior (up to 10^6 cm^{-1}) and a ω^{-4} behavior (for higher frequencies). Raman spectra with the exciting laser beam, polarized parallel to the a+b axis (i.e. perpendicular to stacks), were measured from 100 – 2300 cm^{-1} in a backscattering geometry with a Raman LABRAM HR800 spectrometer equipped with a microscope. Laser line of the 632.8 nm (He-Ne laser) was used with power reduced below 0.1 mW to avoid sample overheating. The spectra were recorded with a spectral resolution of 2 cm^{-1}. Additionally, we have measured room temperature Raman and infrared spectra of neutral donor molecules TCNQ, TCNQF, and TCNQF$_2$. The Raman spectra were recorded for single crystals and the IR spectra for powdered compounds dispersed in KBr pellets.

Variable temperature IR and Raman spectra were measured with the help of a continuous-flow cold-finger cryostat manufactured by Oxford Instruments. A good thermal contact between cold-finger and the sample was achieved using vacuum grease. The spectra were collected at several temperatures from 296 to 8 K. The rate of cooling/heating was 2 K/min.

The complex vibrational features in the optical conductivity and transmittance spectra were decomposed by standard peak fitting techniques that allow extraction of the center frequency and the integral intensity (oscillator strength). The oscillators were fitted using the Voigt spectroscopy function in the PeakFit program [28].

Theoretical calculations for isolated acceptor molecules (TCNQ, TCNQF, and TCNQF$_2$ with charge 0e, -1e) were performed with a software of Gaussian 03W package [29], using the 6-31G(d) basis set and the B3LYP hybrid Hartree-Fock density functional. A geometry optimalization procedure was applied. The results correspond to energy minima and no imaginary frequencies were found. At the level of theory, the C1 symmetry of the molecules

was identified. Vibrational frequencies, infrared intensities, and Raman activities were calculated on the basis of the optimized structure. The Raman activity was transformed to Raman intensity [30]. The results were scaled using the 0.9614 scaling factor [31] since the frequencies computed with a quantum harmonic approximation tend to be higher than experimental ones.

3. Results and discussion

Polarized IR absorption spectra of D_2TCNQF_n (n = 0, 2) single crystals are displayed in Fig. 2. The IR beam was perpendicular to the best-developed *ab* crystal face, which is parallel to donor-acceptor slabs. Since the mixed stacks have the structure …DADDAD…, two CT transitions of the type donor-acceptor (D→A) and donor-donor (D→D) are expected. Taking into account the modes of overlap between molecules inside and between trimers [5], we assume that the energy of D→A transition should be lower than that one of D→D. The assumption is confirmed by polarization of the D→A band (see below).

3.1 Electronic spectra

For the neutral D_2TCNQ complex (n=0), for the electrical vector polarized along the donor-acceptor stacks (E ∥ *a-b*) the IR spectrum shows a broad electronic absorption; on closer examination one can distinguish that this absorption consists of two strongly overlapping electronic excitations at about 4200 and 5500 cm^{-1} (Fig. 2a), which can be assigned to CT transitions D→A and D→D, respectively. The complex is essentially neutral but, because of the overlap between planar molecules within the stacks, a small CT interaction should be possible. In the E ∥ *a-b* spectrum one can distinguish only a few weak vibrational features. For the perpendicular polarization (E⊥*a-b*) two analogous electronic bands are observed (though of lower intensity) and a series of vibrational features, mostly attributed to IR active modes of D and A molecules. We assume that for E⊥*a-b* the electronic bands mainly correspond to side-by-side CT transitions between stacks, though a contribution of intra-stack transitions cannot be excluded because the molecular planes are not exactly perpendicular to the stacking axis. It is important to emphasize that the electronic spectrum of D_2TCNQ complex essentially does not exhibit significant anisotropy.

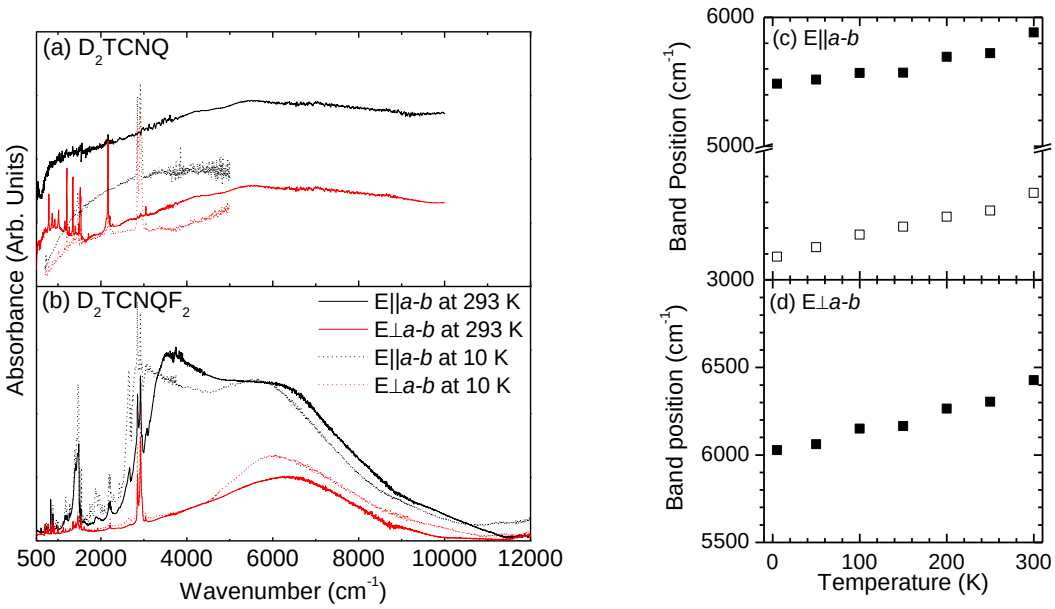

Figure 2. IR absorbance spectra of D_2TCNQ (a), and D_2TCNQF_2 (b) single crystals for polarization parallel (E ‖ *a-b*) and perpendicular (E⊥*a-b*) to donor-acceptor stacks; temperature dependence of position of (c) charge-transfer band components in spectra D_2TCNQF_2 polarized E||*a-b* and (d) maximum of charge-transfer band in spectra D_2TCNQF_2 polarized E⊥*a-b* (adapted from Ref. [32]).

For the ionic D_2TCNQF_2 complex (n=2), the absorption spectra exhibit remarkable anisotropy (Fig. 2b). For polarization parallel to the stacks (E ‖ *a-b*), the spectra display two electronic excitations centered at about 3600 and 6150 cm^{-1} (at 293 K). We attribute these bands to the intra-stack D→A and D→D transitions, respectively. Temperature dependence of the CT components are presented in Fig. 2c. For polarization E⊥*a-b*, only one band centered at about 6350 cm^{-1} is clearly seen. This band should be mainly related to inter-stack CT within the *ab* plane, however it is possible that, due to stack geometry, the intra-stack CT has also a contribution for this polarization (note a difference of about 200 cm^{-1} in comparison with E ‖ *a-b*). Temperature dependence of maximum of the CT-band is presented on Fig. 2d. For both polarizations one can see many vibrational features which are discussed below. Polarization of the D→A band supports our above assumption about its origin.

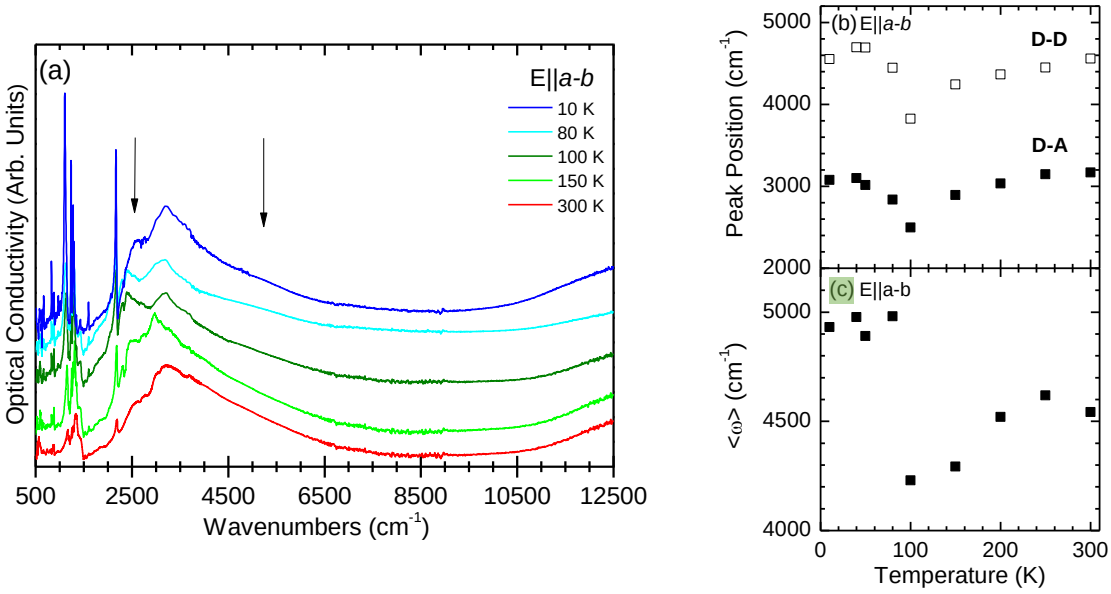

Figure 3. (a) Optical conductivity spectra of D_2TCNQF single crystal, polarized along the stacks for variable temperatures (Adapted with permission from {J. Phys. Chem. C **120**, 23740–23747 (2016)}. Copyright {2016} American Chemical Society); (b) positions of maxima of electronic bands D→A and D→D (see text); (c) center of the spectral weight <ω> calculated for the optical conductivity spectra for E//a-b in the frequency range 1500-10000 cm^{-1}.

For both polarizations the electronic bands of D_2TCNQ (n=0) and D_2TCNQF_2 (n=2) complexes do not exhibit any important changes down to T=10 K (Fig. 2). On the other hand, on temperature decreasing, the electronic bands of D_2TCNQF complex (n=1) undergo significant modifications (Fig. 3a). In the optical conductivity spectra polarized E ‖ *a-b* at room-temperature the broad electronic absorption (2000-8000 cm^{-1}), centered at about 3600 cm^{-1}, is assigned to a superposition of CT transitions D→A and D→D in mixed stacks, i.e. bands centered at about 3160 and 4600 cm^{-1}, respectively (band deconvolution is presented in Supplementary Information in Fig. S1). Below about 200 K, in the region of strong charge and lattice fluctuations, the spectral density shifts towards lower frequencies but at lowest temperatures the spectrum becomes similar to that one at room temperature. In this region one can also see an additional, rather weak and relatively narrow electronic feature at about 2400 cm^{-1} (this band and the D→D band are marked with arrows in Fig. 3a). Temperature dependence of maxima of the D→A and D→D bands is shown in Fig. 3b – note that within the broad region of N-I transition, the frequencies of both bands are lowered. Center of the spectral weight significantly jumps at ca. 100 K towards higher frequencies (Fig. 3c). However, it changes of only ca. 700 cm^{-1} and still stays in the mid-infrared region at low-temperatures. It indicates that upon cooling the change of electrical properties is relatively small. The maximum of the electronic absorption centered at ca. 3600 cm^{-1} at room-temperature is one of the lowest lying CT electronic transitions within the mixed-stack materials. In TTF-CA that is a prototype material undergoing N-I transition, the analogous band is observed at around 5000 cm^{-1} [33]. In other mixed-stack complexes, the CT band was also observed at higher frequencies: at around 4350 cm^{-1} for (BEDT-TTF)(ClMeTCNQ), at 5800 cm^{-1} for (BEDT-TTF)(Me_2TCNQ),

6290 cm^{-1} for (BEDO-TTF)(Cl_2TCNQ) [34, 35]. Such a low-lying CT-energy band in D_2TCNQF indicates proximity to the N-I boundary and its sensibility to the N-I phase transition. Moreover, it is suggested that presence of absorption band below 5000 cm^{-1} that is related to intermolecular transition in the mixed-valence state indicates a lack of fully ionic nature of such complex [35].

3.2 Vibrational spectra

For a neutral complex, where there is nearly no CT between D and A, the vibrational spectra mostly consist of IR active modes of component neutral molecules (Fig. S2 and Tables S1, S2, S3 in Supplementary Materials). On the other hand, when there exists a certain degree of CT, in the spectra we see not only IR active modes but also some other intensive and broad bands dominating the spectra, which are attributed to the coupling of the totally symmetric modes with the intra-stack CT excitation (EMV coupling). In the case of CT complexes, the frequency of some normally IR active modes (not interacting with electrons) usually depends linearly on the mean charge residing on molecule, therefore these modes are often used for the evaluation of the degree of CT (ρ) [36]. Additionally, it is important to remember that the vibrational features due to EMV coupling can only be observed when the molecules are not located in crystal sites with the inversion symmetry centers, i.e. the EMV effects cannot be seen for perfectly regular stacks because the probability of exchanging electrons with upper and down neighboring molecules is the same. It is important that for an isolated symmetric DAD trimer, which undergoes a N-I transition, a spontaneous symmetry lowering and thus enhancement of non-uniform charge distribution is driven by the EMV coupling. The effect was observed in the complex $(TTF)_2I$•A (acceptor IA=iodanil) in which DAD trimers are isolated and not arranged in stacks. In this complex in its quasi-neutral state the molecules form symmetric trimers but, in its quasi-ionic state, the trimers are distorted [37, 38]. This type of EMV distortion is most expected in the D_2TCNQF complex, all the more because, as mentioned above, the DAD trimers in this complex cannot be treated as exactly centrosymmetrical, due to the fluorine atom positional disorder. Additionally, it should be stressed that, at variance with CT complexes with segregated stacks, in the complexes with mixed D-A stacks also Raman spectra can be affected by EMV interaction. Small electron oscillations between D and A molecules are coupled to the totally symmetric modes of both molecules, therefore the same modes of similar frequency are seen in both IR and Raman spectra [20, 39]. However, the vibronic frequency shift is only expected in the case of partial CT; when $\rho \rightarrow 0$ or $\rho \approx 1$ nearly no frequency shift is expected even though EMV coupling constants are non-zero [39]. All the vibrational bands observed in IR and Raman spectra, together with proposed assignments, are listed in Tables S4, S5 and S6 in Supplementary Materials. The assignment was supported by results of DFT calculations of isolated acceptor molecules (Figs. S2, S3 and Tables S1, S2, S3 in Supplementary Materials).

To simplify the further discussion we assume that most vibrational modes of TCNQF and $TCNQF_2$, especially those related to C≡N or C=C stretching, are similar to those of TCNQ, therefore for all the acceptors, we use the notation of modes as for TCNQ. Room temperature

IR spectra of three studied compounds (n=0,1,2) within the frequency region of strong vibrational features (700-1700 cm^{-1}) are displayed in Fig. 4. It is important that the intensities of absorbance spectra of D_2TCNQ and D_2TCNQF_2 are much lower in comparison with those of D_2TCNQF.

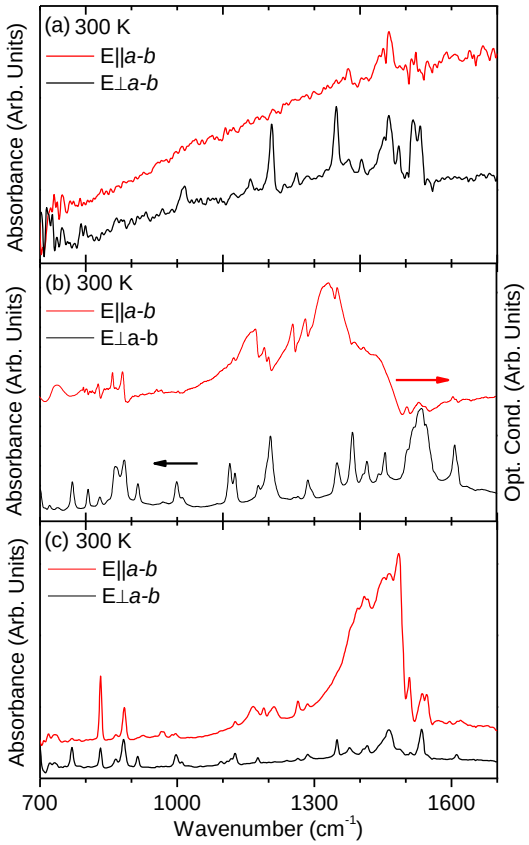

Figure 4. Room temperature IR absorbance spectra of D_2TCNQ (a), optical conductivity spectra of D_2TCNQF (b) (Adapted with permission from {J. Phys. Chem. C **120**, 23740–23747 (2016)}. Copyright {2016} American Chemical Society), and absorbance spectra of D_2TCNQF_2 (c) single crystals for polarization parallel (E ‖ *a-b*) and perpendicular (E⊥*a-b*) to donor-acceptor stacks.

3.2.1 Acceptor C≡N stretching modes

The TCNQ molecule has three normal modes related to C≡N stretching; for neutral molecule $TCNQ^0$: $\nu_2(a_g)$ = 2229 cm^{-1}, ν_{19} (b_{1u}) = 2228 cm^{-1} and ν_{33} (b_{2u}) = 2228 cm^{-1} [40]. In the CT complexes the totally symmetric $\nu_2(a_g)$ mode interacts with electrons, therefore its frequency is not good for evaluation of the degree of CT. The frequency of the IR active mode ν_{19} (b_{1u}) is located in a spectral region relatively free from other vibrations and its frequency depends linearly on the mean charge residing on the molecule (it shifts down to 2181 cm^{-1} for $TCNQ^-$ [40]), therefore this mode was often used for determination of the degree of CT. However, a correct assignment of this mode is sometimes doubtful and first of all it is sensitive to interactions with neighboring molecules. It is possible that in our complexes the donor-acceptor halogen bonding has a considerable influence on the C≡N modes, therefore the ν_{19}

(b_{1u}) mode may be not suitable for evaluation of the charge density (similarly the ν_{33} (b_{2u}) mode). On the other hand, the C≡N modes can be useful to analyze donor-acceptor interactions and halogen bonding interactions.

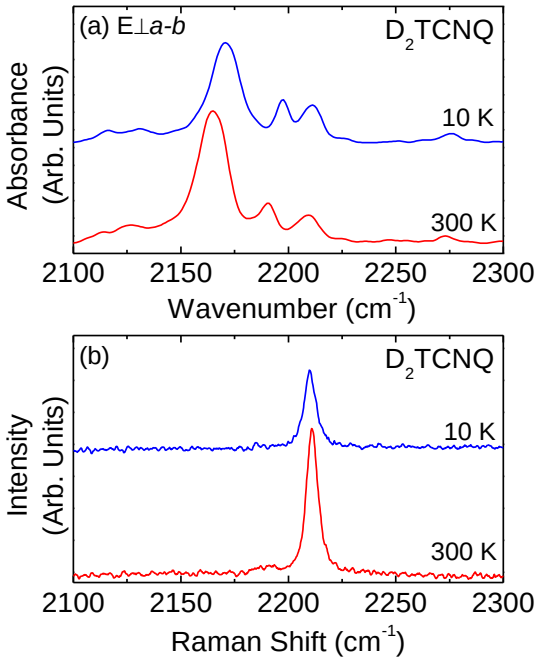

Figure 5. (a) Infrared absorbance spectra of D_2TCNQ single crystals for T = 10 and 300 K for polarization perpendicular (E⊥*a*-*b*) to donor-acceptor stacks (adapted from Ref. [32]); (b) Raman spectra of D_2TCNQ single crystals for T = 10 K and 300 K for $\lambda_{exc.}$= 632.8 nm.

For the D_2TCNQ complex (n=0) in both polarizations, we observe a band at 2165 cm^{-1} at 300 K (2171 cm^{-1} at 10 K), which is assigned to the coupling of $\nu_2(a_g)$ TCNQ mode with electrons. The shift of this mode towards lower frequency in IR spectra (by about 64 cm^{-1} in comparison with neutral TCNQ) gives evidence of the EMV coupling, nevertheless the halogen bonding can also influence the band position. As mentioned above, because of π-π stacking interaction between D and A it should exist a small CT interaction. Presence of the EMV coupling means that the centrosymmetric trimer is slightly distorted (see below). Since this band is only seen as a rather weak vibrational feature for polarization E∥*a*-*b*, in Fig. 5a we display only the C≡N modes for polarization E⊥*a*-*b*. The $\nu_2(a_g)$ band in Raman spectrum is observed at 2210 cm^{-1} at 300 K (Fig. 5b), i.e. it is not affected by EMV coupling, as expected for ρ≈0. Two IR bands at 2210 and 2191 cm^{-1} (at 300 K) are assigned to the IR active ν_{19} (b_{1u}) and ν_{33} (b_{2u}) modes, respectively.

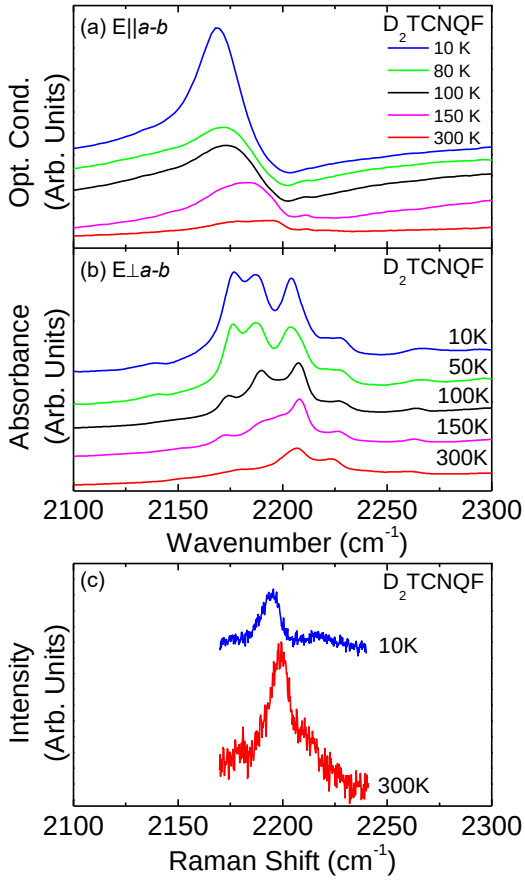

Figure 6. Temperature dependence of IR spectra of D_2TCNQF single crystal: optical conductivity spectra (a) for polarization E ‖ *a-b* and absorbance spectra (b) for polarization E⊥*a-b* (adapted with permission from Ref. [5]); Raman spectrum of single crystal (c) for T = 10 and 300 K ($\lambda_{exc.}$= 632.8 nm).

The IR spectra of D_2TCNQF complex (n=1) within the region of C≡N stretching for two polarizations are displayed in Figs 6a and 6b, along with the Raman spectrum in Fig. 6c. As previously suggested in Ref. [5], the acceptor $\nu_2(a_g)$ mode is evidently coupled with electrons. In the IR spectrum at 300 K for polarization E ‖ *a-b* , this mode is observed as a strong band which consists of two components at 2182 and 2194 cm^{-1} (Fig. 6a). On the other hand, the $\nu_2(a_g)$ mode in the Raman spectrum is seen at 2199 cm^{-1} at 300 K and shifts down to 2194 cm^{-1} at 10 K – the mode is also evidently affected by EMV interaction, as expected for complex with mixed stacks and partial CT. Activation of the $\nu_2(a_g)$ mode in IR spectrum indicates that acceptors are not precisely located in the center of symmetry. Most probably the acceptor position fluctuates around (or is slightly shifted from) the center of symmetry, i.e. at least in the time-scale of vibrational spectroscopy the DAD trimer is distorted. Such distortion is enhanced by the EMV coupling, as was shown for isolated DAD trimers undergoing a N-I transition [37, 38]. When the small distortion is static, it is reasonable to assume that its direction can be different in different trimers. Most probably there exist trimers with up and down distortions against the center of symmetry. It is also possible that in the crystal exist two kinds of domains: with up and down trimer distortions. On cooling, when the degree of CT increases, the effect of EMV distortion also increases [37, 38], therefore the size of trimer distortion, and thus a non-uniformity of charge distribution should increase significantly. Consequently, the intensity of

the $\nu_2(a_g)$ band strongly increases and it shifts towards lower frequency; in the conductivity spectrum at 10 K for E ‖ *a-b*, we see essentially a single peak at 2167 cm^{-1}. The distortion of DAD trimers in D_2TCNQF complex is largely yielded by EMV coupling, though the situation is more complicated than in $(TTF)_2$•IA complex [37, 38] since trimers are not isolated but arranged in stacks. For perpendicular polarization E⊥*a-b*, the IR absorption spectra exhibit a strong vibrational feature consisting of two components (2175 and 2188 cm^{-1} at 10 K). These peaks are also assigned to the $\nu_2(a_g)$ mode activated by the EMV coupling. Evidently, since molecular planes are not exactly perpendicular to the stacking axis, the strong $\nu_2(a_g)$ band is also well seen in the IR spectra for perpendicular polarization. The bands at 2224 and 2207 cm^{-1} (at 300 K) in the IR absorption spectra for E⊥*a-b* were assigned to ν_{19} (b_{1u}) and ν_{33} (b_{2u}), respectively (Fig. 6b).

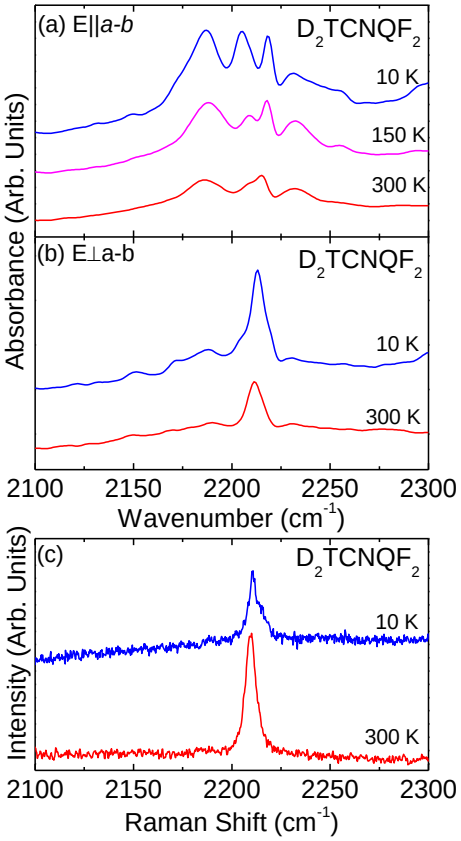

Figure 7. Temperature dependence of IR absorbance spectra of D_2TCNQF_2 single crystal polarized parallel (a) and perpendicular (b) to donor-acceptor stacks; (c) single crystal Raman spectra for T = 10 and 300 K for $\lambda_{exc.}$= 632.8 nm (adapted from Ref. [32]).

The IR spectra of D_2TCNQF_2 complex (n=2) within the region of C≡N stretching are presented in Figs 7a and 7b, and Raman spectrum in Fig. 7c. For polarization E ‖ *a-b*, the $\nu_2(a_g)$ IR band being a consequence of EMV coupling is seen at 2186 cm^{-1} at 300 K, however, in contradiction with in D_2TCNQ (n=0) and D_2TCNQF (n=1) complexes, this mode is hardly detectable for polarization E⊥*a-b*. The $\nu_2(a_g)$ mode in Raman spectrum is observed at 2210 cm^{-1} (at 300 K) – it is not shifted by vibronic effect. Both the ν_{19} (b_{1u}) and ν_{33} (b_{2u}) modes are quite well identified in IR spectrum for E ‖ *a-b*. At 300 K, the ν_{33} (b_{2u}) mode consists of two components at 2209 and 2016 cm^{-1}; the lower frequency one strongly grows on cooling down

(Fig. 7a). For E⊥*a-b*, the IR spectrum is dominated by the ν_{33} (b_{2u}) mode at 2211 cm^{-1} while the ν_{19} (b_{1u}) mode at 2234 cm^{-1} is much weaker (Fig. 7b).

The three studied complexes are isostructural however, their IR spectra exhibit interesting differences within the C≡N modes. The $\nu_2(a_g)$ mode is activated in IR spectra due to EMV coupling, therefore its position is shifted towards lower frequency. This activation of the $\nu_2(a_g)$ mode in IR spectrum gives evidence that DAD trimers are not exactly centro-symmetrical or that the positions of acceptors slightly fluctuate around the center of symmetry. This effect is especially strong for D_2TCNQF. Due to the strong D-A interactions arising from halogen bonding, the IR active ν_{19} (b_{1u}) and ν_{33} (b_{2u}) modes are not effective for evaluating the degree of charge transfer (CT). The EMV coupling has also an influence on the $\nu_2(a_g)$ Raman band but only for D_2TCNQF, as expected for complex with intermediate degree of CT. The C≡N bands observed in IR and Raman spectra are listed in Tables I and II, respectively.

3.2.2 Acceptor and donor C=C stretching and C-H bending modes

Within the region of C=C stretching, the IR spectra of D_2TCNQ and D_2TCNQF_2 complexes are dominated by bands attributed to donor modes, while the spectra of D_2TCNQF complex by acceptor modes. Taking into account that in CT complexes the C=C modes of TCNQ (or its fluorinated derivatives) strongly interact with electrons thus yielding the strongest IR bands, one can suggest that a dominating CT excitation, which is involved in EMV coupling, occurs in D_2TCNQ (n=0) and D_2TCNQF_2 (n=2) complexes between donors but in D_2TCNQF (n=1) complex between donor and acceptor. The partial CT in D_2TCNQF should play an important role in this difference.

Within the region of C=C stretching, the TCNQ molecule has two totally symmetric modes: $\nu_3(a_g)$ =1602 cm^{-1} and $\nu_4(a_g)$ = 1454 cm^{-1} for neutral $TCNQ^0$ molecule . For the $TCNQ^-$ anion the $\nu_3(a_g)$ mode is shifted towards the higher frequency by 13 cm^{-1} and the $\nu_4(a_g)$ mode towards the lower frequency by 63 cm^{-1} [40]. It is well known that in TCNQ salts both C=C modes strongly interact with electrons yielding intensive broad bands strongly shifted towards lower frequencies. Also the C-H bending mode $\nu_5(a_g)$ = 1207 cm^{-1} (for $TCNQ^0$) shows the strong EMV coupling [18]. On the other hand, the donor EDT-TTF-I_2 has three vibrational modes related with C=C stretching: $D\nu_5$ =1552 cm^{-1}, $D\nu_6$ = 1515 cm^{-1}, and $D\nu_7$ = 1492 cm^{-1} for the neutral molecule [41]. It should be noticed that in vibrational spectra of the three studied compounds the C=C donor and acceptor modes can overlap.

Temperature dependence of IR absorbance spectra of D_2TCNQ (n=0) complex is shown in Figs 8a and 8b, and the Raman spectra in Fig. 8c. A relatively broad and rather weak vibrational feature in the IR spectra, centered at about 1460 cm^{-1} (doublet 1460 and 1451 cm^{-1}) is quite well seen in both polarizations. We assign this band to the effect of EMV coupling of the donor C=C stretching modes with electrons. For polarization E ∥ *a-b* the C=C modes couple with intra-stack CT between D molecules but for E⊥*a-b* they should be mainly coupled with inter-stack CT, nevertheless an intra-stack contribution is also possible. An analogous broad band at about 1424 cm^{-1} (doublet 1432 and 1412 cm^{-1}) is observed in Raman spectrum (Fig. 8c). In comparison with the C=C modes of neutral donor, the position of C=C Raman band in the

complex is strongly shifted towards lower frequency and it is remarkable that its position is very close to the analogous IR band. Evidently, the EMV coupling has also an influence on the position of Raman band in this complex.

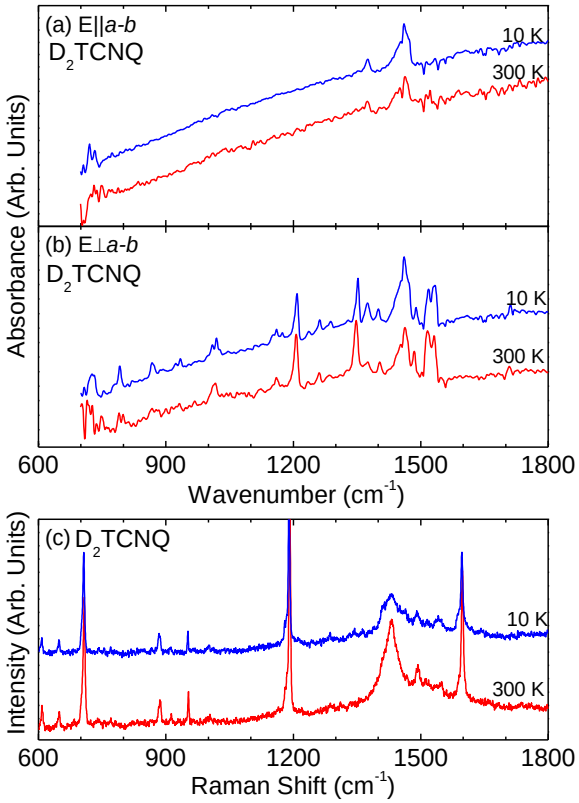

Figure 8. IR absorbance spectra of D_2TCNQ single crystals for polarization parallel (a) and perpendicular (b) to donor-acceptor stacks for T = 10 and 300 K. (c) Raman spectra of D_2TCNQ for T = 10 and 300 K for $\lambda_{exc.}$= 632.8 nm (adapted from Ref. [32]).

At room temperature, in the IR spectrum of D_2TCNQF (n=1) complex for polarization E ∥ *a-b*, the acceptor $\nu_3(a_g)$ mode is observed at 1599 cm^{-1} (Fig. 9a). The presence of antiresonance dip in CT band, which is better seen in the reflectance spectrum (Fig. S4), provides convincing evidence of the EMV interaction. On temperature decreasing the relative intensity of the $\nu_3(a_g)$ mode strongly grows but its position does not change significantly (1598 cm^{-1} at 8 K). Since molecular planes are not exactly perpendicular to the stacking axis, the $\nu_3(a_g)$ mode is also present for polarization for E⊥*a-b*. It is clearly seen that at room temperature it consists of two lines at 1607 and 1613 cm^{-1} which we assign to $TCNQF^0$ and $TCNQF^-$, respectively (Fig. 9b). Within the time-scale of IR spectroscopy the acceptors with higher and lower charge densities (as determined from X-ray data) can be observed as ions $TCNQF^-$ and neutral $TCNQF^0$ molecules, respectively. This happens when the time-of-life of the $TCNQF^-$ ion (and thus $TCNQF^0$) is much longer than the vibrational period of $\nu_3(a_g)$ mode. The intensities of both components grow on temperature decreasing (Fig. 9b), however the intensity of $TCNQF^-$ line at 1613 cm^{-1} grows stronger. Due to the N-I transition, the number of the $TCNQF^-$ ions increases – obviously, if they are observed in the time-scale of IR spectroscopy. In Raman

spectrum we find two bands at 1612 and 1607 cm^{-1} supporting thus the above discussion of IR features (Fig. 9c).

In the IR spectrum of D_2TCNQF for E ‖ *a-b*, we observe two EMV bands which can be assigned to the $\nu_4(a_g)$ C=C stretching mode: at room temperature a relatively narrow band at 1356 cm^{-1} ($TCNQF^{-}$) and a relatively broad band at 1336 cm^{-1} ($TCNQF^0$). On cooling the intensity of both bands strongly grows. A similar effect is observed for the $\nu_5(a_g)$ mode which is mostly related to the EMV coupling of the ring C-H bending vibrations. However, in the spectral range of the $\nu_5(a_g)$ mode, a C-F stretching mode (around 1250 cm^{-1}) is also present since in TCNQF molecule one of H atoms is replaced by F atom. The C-F stretching frequency is close to the frequency of the $\nu_5(a_g)$ mode (1273 cm^{-1} in $TCNQF_4$ [42]), nevertheless, in order to simplify the discussion, we assume that bands at 1256 cm^{-1} and 1173 cm^{-1} are mostly related to C-H bending of $TCNQF^{-}$ and $TCNQF^0$. It is obvious that the C-F stretching should be hardly seen for the E ‖ *a-b* polarization. At room temperature a band at 1256 cm^{-1} is assigned to the $\nu_5(a_g)$ of $TCNQF^{-}$ and a band at 1173 cm^{-1} to the $\nu_5(a_g)$ of $TCNQF^0$. Analogous splitting of the $\nu_4(a_g)$ and the $\nu_5(a_g)$ modes was observed in 2:1 TCNQ salts with tetramerized …ABBA… segregated stacks, with non-uniform charge distribution between molecules in tetramers (e.g. $A^{0.4e}$ and $B^{0.6e}$ as determined from X-ray TCNQ bond lengths) [18, 43, 44]. However, in these tetramerized TCNQ salts, the splitting was present for all the a_g modes which exhibit a strong EMV coupling, i.e. not only for $\nu_4(a_g)$ and $\nu_5(a_g)$ modes but also for $\nu_2(a_g)$ and $\nu_3(a_g)$ modes. Notwithstanding, in the TCNQF complex investigated here, the $\nu_2(a_g)$ and $\nu_3(a_g)$ are also doublets though the splitting is not so spectacular. Additionally, in the IR spectrum of D_2TCNQF for E ‖ *a-b* (Figs 4 and 9a) we see a band at 1438 cm^{-1} (at 300 K) which can be attributed to the EMV coupling of donor C=C modes, however the intensity of this vibrational feature is much lower in comparison with TCNQF bands (see also Fig. S4). It should be emphasized that the proposed assignment of doublets related to the $\nu_4(a_g)$ and $\nu_5(a_g)$ modes is based on analogy with IR spectra of tetramerized TCNQ salts [18, 43, 44]. The EMV coupling effects for both donor and acceptor modes are also well seen in Raman spectra (Fig. 9c). The broad Raman bands consisting of several lines and centered at about 1369 and 1187 cm^{-1} are related to the $\nu_4(a_g)$ and $\nu_5(a_g)$ modes, respectively. Additionally, we see also a relatively weaker Raman band centered at 1446 cm^{-1} attributed to the donor C=C stretching modes which are also coupled with electrons.

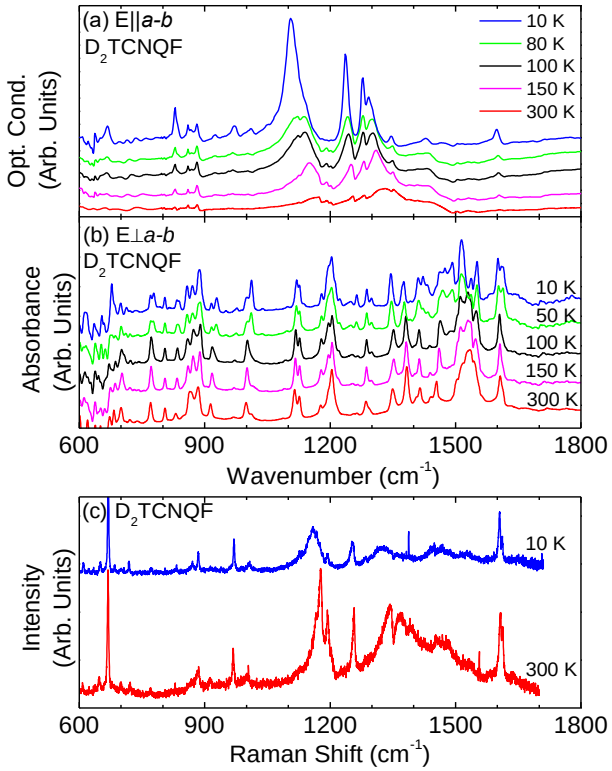

Figure 9. IR optical conductivity spectra of D_2TCNQF single crystals for polarization (a) parallel to donor-acceptor stacks and IR absorbance spectra of $(EDT\text{-}TTF\text{-}I_2)_2TCNQF$ single crystals for polarization (b) perpendicular to the stacks for variable temperatures. (c) Raman spectra of D_2TCNQF for T = 10 and 300 K for $\lambda_{exc.}$= 632.8 nm (Adapted with permission from {J. Phys. Chem. C **120**, 23740–23747 (2016)}. Copyright {2016} American Chemical Society.).

IR absorbance and Raman spectra of D_2TCNQF_2 (n=2) complex are presented in Fig. 10. In the IR spectrum, a broad band centered at about 1460 cm^{-1} is seen in both polarizations, though its intensity for E$\|$*a-b* is stronger (the shape is also different) than for E$\perp$*a-b*. We assume that it is a spectral effect of EMV coupling with intra-stack CT transitions between donor molecules (Fig. 10a). However, it is possible that for E$\perp$*a-b* the side-by-side CT between donors in neighboring stacks plays a much more significant role (Fig. 10b). In the Raman spectrum at 300 K we see an analogous broad spectral feature consisting of two lines at 1432 and 1411 cm^{-1}, which we attribute to the C=C donor modes (Fig. 10c).

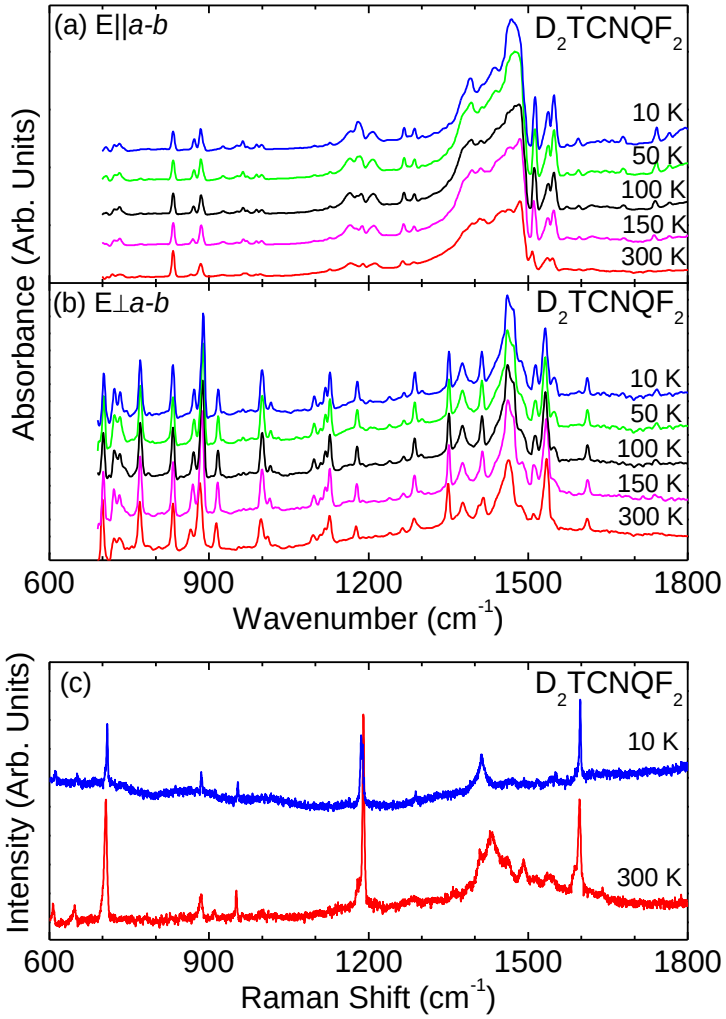

Figure 10. Infrared absorbance spectra of D_2TCNQF_2 single crystals for polarization (a) parallel and (b) perpendicular to donor-acceptor stacks for variable temperatures. (c) Raman spectra of D_2TCNQF_2 for T = 10 and 300 K for $\lambda_{exc.}$= 632.8 nm (adapted from Ref. [32]).

Now we discuss IR active modes which are mostly observed for perpendicular polarization E⊥*a*-*b*. In the region of C=C stretching, there exists the $\nu_{20}(b_{1u})$ TCNQ mode whose position depends linearly on the charge density on molecule (1545 cm^{-1} for $TCNQ^0$ and 1504 cm^{-1} for $TCNQ^-$ [40]) . Usually, this mode gives more reliable values of charge density than the C≡N modes since it is less sensitive to interactions with neighboring molecules. It should be also noted that in our complexes the identification of $\nu_{20}(b_{1u})$ mode is not easy since it is located in the spectral region of donor C=C stretching. Moreover, at a lower frequency, the $\nu_{21}(b_{1u})$ mode, which is charge sensitive (1405 cm^{-1} for $TCNQ^0$ and 1361 cm^{-1} for $TCNQ^-$ [40]), is also observed.

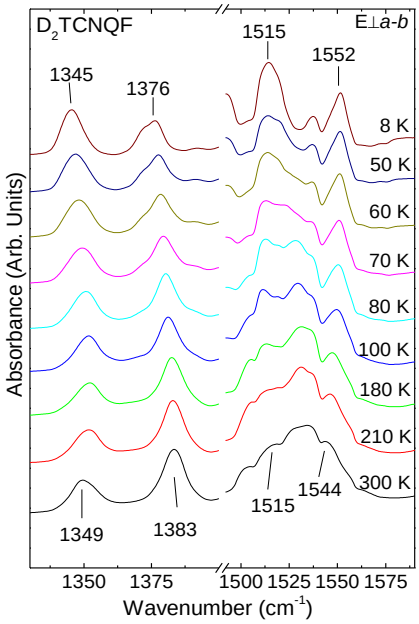

Figure 11. Temperature dependence of $\nu_{20}(b_{1u})$ and $\nu_{21}(b_{1u})$ modes in IR spectrum of D_2TCNQF for polarization E⊥*a-b* (Adapted with permission from {J. Phys. Chem. C **120**, 23740–23747 (2016)}. Copyright {2016} American Chemical Society.)

At room temperature, in the IR spectrum of D_2TCNQF complex for polarization E⊥*a-b*, we see two bands at 1515 and 1544 cm^{-1} which can be assigned to $\nu_{20}(b_{1u})$ mode of $TCNQF^{-}$ and $TCNQF^{0}$, respectively (Figs 9b and 11). On cooling the intensity of both bands increases but the intensity of $TCNQF^{-}$ band grows much stronger than for $TCNQF^{0}$, as expected from the N-I transition. Obviously, the proposed assignment assumes that, as discussed above, the lifetime of $TCNQF^{-}$ anions is long enough in comparison with the time-scale of IR spectroscopy. Similar behavior is seen for the $\nu_{21}(b_{1u})$ mode: at room temperature we find two bands at 1349 and 1383 cm^{-1} that can be attributed to $TCNQF^{-}$ and $TCNQF^{0}$, respectively. As expected, on cooling the intensity of $TCNQF^{-}$ band grows stronger than the intensity of $TCNQ^{0}$ band (Figs 9a and 11).

The $\nu_{20}(b_{1u})$ and $\nu_{21}(b_{1u})$ modes are also well seen in IR spectra of D_2TCNQ and D_2TCNQF_2 complexes for polarization E⊥*a-b*. In the D_2TCNQ complex we find two bands related to neutral $TCNQ^{0}$: the band at 1532 cm^{-1} can be assigned to the $\nu_{20}(b_{1u})$ mode and the band at 1348 cm^{-1} to the $\nu_{21}(b_{1u})$ mode (Fig. 8b). Similarly, in IR spectrum of the $TCNQF_2$ complex, we observe two bands of $TCNQF_2^{-}$: the band at 1534 cm^{-1} is related to the $\nu_{20}(b_{1u})$ mode and the band at 1349 cm^{-1} to the $\nu_{21}(b_{1u})$ mode (Fig. 10b).

As already discussed above, in the spectra of D_2TCNQ and D_2TCNQF_2 complexes, the dominating EMV bands are related to donor vibrations. However, on closer examination in the IR spectrum of D_2TCNQF_2 complex for E∥*a-b*, we find three weak bands at 1211, 1190 and 1167 cm^{-1} (at 300 K) which can be attributed to the effect of EMV interaction of $\nu_5(a_g)$ mode (Fig. S5). It means that in the D_2TCNQF_2 complex, there is also a small EMV coupling with D→A charge transfer excitation. All the discussed above bands observed in IR and Raman spectra are listed in Tables I and II, respectively.

Table I. Selected vibrational bands in room temperature IR spectra of D_2TCNQF_n (n=0,1,2) complexes, $TCNQF_n$ acceptors (A), donor (D)

D_2TCNQ		D_2TCNQF		D_2TCNQF_2		$TCNQ^0$ [40]	$TCNQ^-$ [40]	IR $TCNQF^0$	IR $TCNQF_2{}^0$	D^0 [41]	Assignment $TCNQ^0/D^0$
Abs. ∥	Abs.⊥	Cond.∥	Abs.⊥	Abs. ∥	Abs.⊥						
- -	2209 2190	- -	2223 2207	2232 2215 2210	2231 2212	2228 2228	2181 2153	2223 2217	2230 2219	- -	A $\nu_{19}(b_{1u})$ A $\nu_{33}(b_{2u})$
- 2166	- 2166	2195 2178	- 2181	- 2186	- 2190	2229	2206	-	-	-	A $\nu_2(a_g)$ EMV
-	-	1605	1613 1607	1615 1620	1611	1602	1615	1617	1599	-	A $\nu_3(a_g)$ EMV
1533	1532	-	1543 1534	1536 1546	1535	1545	1504	1557	1576	-	A $\nu_{20}(b_{1u})$
-		1530	1543 1534			1540	1518	1549	1550	-	A $\nu_{34}(b_{2u})$?
1463	1463	1436	1440 1455 1504	1464 1453	1464 1446	-	-	-	-	1552 1515 1492	D C=C stretch. EMV
-	1403	-	1407 1415	1417 1410	1415 1409	1405	1361	1390	1393	1407	A$\nu_{21}(b_{1u})$
1348	1348	1352	1349	-	1349	1354	1388	1353	1363	-	A $\nu_{35}(b_{2u})$
- -	- -	1352 1332	- -	- -	- -	1454	1391	1446	-	-	A $\nu_4(a_g)$ EMV
- - -	- - -	1255 1173 1125	- - -	1212 1189 1166	- - -	1207	1196	-	-	-	A ν_5 (a_g) EMV

Table II. Selected vibrational bands in room temperature Raman spectra of D_2TCNQF_n (n=0,1,2) complexes, $TCNQF_n$ acceptors (A), donor (D)

D_2TCNQ (cm^{-1})	D_2TCNQF (cm^{-1})	D_2TCNQF_2 (cm^{-1})	$TCNQ^0$ [40] (cm^{-1})	Raman $TCNQF^0$ (cm^{-1})	Raman $TCNQF_2{}^0$ (cm^{-1})	D^0 [41] (cm^{-1})	Assignment $TCNQ^0/D^0$
2211	2211 2199	2210	2229	2223	2233	-	A $\nu_2(a_g)$
1598 -	1612 1608	1597 -	1602	1620	1636	-	A $\nu_3(a_g)$
1461	1457	1461	1456	1461	1460	-	A $\nu_4(a_g)$
1431 1412	1442 -	1431 1409	- -	-	-	-	D C=C EMV
- - -	1392 1369 1344	- - -	1456	1461	1460	-	A $\nu_4(a_g)$ EMV
-	1257	1283	-	1263	1263	-	A C-F stretch.
- -	1167 1177	- -	1187 -	1182 -	1184 -	- -	A $\nu_5(a_g)$ EMV

3.3. Temperature dependence of structural parameters

For analysis of EMV coupling phenomena in the studied compounds, it is essential to have knowledge of the most important interactions both inside and between trimerized stacks and their modifications as a function of temperature. For this reason, using the available crystallographic data [5], we have performed calculations of the most important distances between adjacent molecules. We identified numerous intermolecular contacts shorter (or comparable) than the sum of van der Waals radii as well as noticed some interesting structural modifications on cooling.

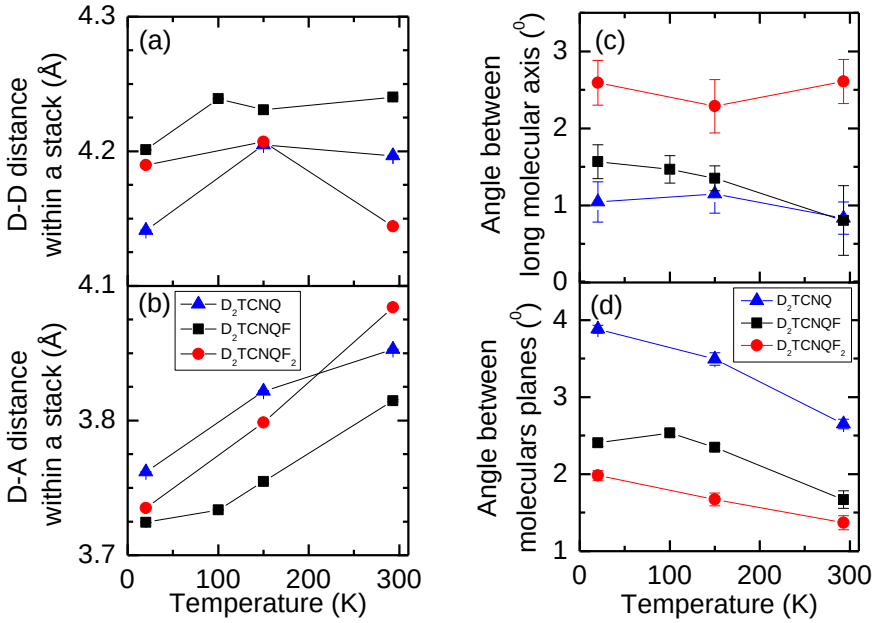

Figure 12. Left: temperature dependence of the distances between centroids of (a) donor molecules (within a dyad) and (b) donor and acceptor molecules within a stack in D_2TCNQF_n (n = 0, 1, 2) complexes for several temperatures. Right: temperature dependence of (c) the angle between long molecular axis of neighboring D and A molecules and (d) angle between D and A molecular planes.

Donor-donor (Figs. 12a, S6b, S7c, S7d, S9f) and donor-acceptor distances (Figs. 12b, S6a, S7a, S7b, S9e) in the D_2TCNQ, D_2TCNQF, and D_2TCNQF_2 complexes are presented for several temperatures. Figure 12c shows temperature dependence of the angle between long molecular axis of neighboring donor and acceptor molecules within a stack. For D_2TCNQ and D_2TCNQF, the angle increases gradually upon cooling. On the other hand, the angle for D_2TCNQF_2 is essentially temperature-independent. Moreover, it is around two-times larger than the angle for D_2TCNQ and D_2TCNQF. It is known that in mixed-stacked CT complexes, orientation of molecular long axes of donor and acceptor within a stack is not parallel [40]. It's related to symmetry of donor and acceptor molecular orbitals and it's a characteristic feature of mixed-stacked CT complexes. It points the fact that structure in the mixed stack material is highly sensitive to subtle changes of relative distance and orientation of molecular partners. The largest rotation angle could contribute to the phase transition. On the other hand, the rotation of molecular axis observed in D_2TCNQF_2 indicates that CT interaction in D_2TCNQF_2 is probably stabilized upon cooling. Figure 12d shows temperature dependence of the angle between

molecular planes of donors and acceptors. Upon cooling, this angle increases for all three complexes. However, the angle value as well as its change as a function of temperature is largest for the neutral complex D_2TCNQ and smallest for the fully ionized complex D_2TCNQF_2. It is suggested that the angle changes mainly in the case of a complex that is formed by neutral or almost neutral molecules.

A detailed examination of the molecules organization in these isostructural series of D_2TCNQ, D_2TCNQF, and D_2TCNQF_2 yields more several distinct relations between molecules depending on whether a 2:1 complex undergoes NIT or not (Figs. S6-S9). These dependences of structure parameters agree well with the spectroscopic results so far. Two of the most important temperature dependences of structure parameters are related to short-contacts (when the distance between atoms is smaller than the sum of van der Waals radii). Temperature dependences of selected short-contacts show that: (a) between neighboring stacks, sulphur-sulphur short contacts are the strongest in D_2TCNQF_2 (Fig. S8g) that agrees with relatively stronger side-by-side interaction (Figs. 2b, S7b and S7c), (b) within a stack, the strongest carbon-sulphur interaction between donor and acceptor molecules is observed in the NIT-complex (Fig. S9e).

4. Conclusions

The IR and Raman spectra of isostructural mixed-stack complexes D_2TCNQF_n (n = 0, 1, 2) provide convincing evidence of strong coupling between electrons and intramolecular vibrations (EMV coupling) in these compounds. Existence of these effects indicates that the trimeric DAD units forming the mixed stacks cannot be exactly centrosymmetric, as was suggested by X-ray crystallographic studies. Previous studies of the isolated centrosymmetric DAD trimers undergoing a N-I phase transition showed that, when the degree of CT between D and A grows, the EMV coupling strongly enhances the asymmetry of charge distribution [37, 38]. It means that the coupling plays an important role in N-I transition. The strong EMV effect observed in IR spectra in D_2TCNQF strongly confirm this suggestion – when the degree of CT increases, the intensities of the EMV bands related to TCNQF molecules strongly increase , i.e. DAD trimers become more distorted. Simultaneously, the EMV effect has a significant influence on Raman spectra of this compound, as expected for mixed stacks with partial charge distribution. On the other hand, the EMV effects in the two other studied compounds (n=0,2) are not so strong, nevertheless they are well seen in IR spectra. At variance with D_2TCNQF, where the EMV effect is dominated by TCNQF vibrations, in complexes D_2TCNQF_n (n = 0, 2) the effect is observed for C=C stretching of D molecule. The reason for this behavior can be related to the fact that for n=0 the complex is essentially neutral and for n=2 a full CT exists, i.e. there is no change of the degree of CT. The EMV coupling effects are much weaker in vibrational spectra of complexes for n = 0, 2, in agreement with theoretical results [39] that these effects are nearly absent (or are weak) when $\rho \rightarrow 0$ or $\rho \rightarrow 1$.

References

1. S. Horiuchi, R. Kumai, Y. Okimoto, Y. Tokura, Chem. Phys. **325**, 78-91 (2006)
2. F. Delchiaro, A. Girlando, A. Painelli, A. Bandyopadhyay, S. K. Pati, G. D'Avino, Phys. Rev. B **95**, 1555125 (2017)
3. S. Tomić and M. Dressel, Rep. Prog. Phys. **78**, 096501 (2015)
4. R. C. Wheland, J. Am. Chem. Soc. **98**, 3916 (1976)
5. J. Lieffrig, O. Jeannin, A. Frąckowiak, I. Olejniczak, R. Świetlik, S. Dahaoui, E. Aubert, E. Espinosa, P. Auban-Senzier, M. Fourmigué, Chem. Eur. J. **19**, 14804–14813 (2013)
6. L. R. Melby, R. J. Harder, W. R. Hertler, W. Mahler, R. E. Benson and W. E. Mochel, J. Am. Chem. Soc. **84**, 3374-3387 (1962)
7. J. P. Ferraris, G. Saito, J. Chem. Soc. Chem. Commun. 992-993 (1978)
8. G. Saito, J.P. Ferraris, J. Chem. Soc. Chem. Commun. 1027-1029 (1979)
9. T.J. Enge, D.O. Cowan, A.N. Bloch, and T.J. Kistenmacher, Mol. Cryst. Liq. Cryst. **95**, 191 (1983)
10. T. Murata, K. Nakamura, H. Yamochi, G. Saito, Synth. Met. **159**, 2375-2377 (2009)
11. T. Hasegawa, S. Kagoshima, T. Mochida, S. Sugiura and Y. Iwasa, Solid State Comm. **103**, 489-493 (1997)
12. T. J. Emge, F. M. Wiygul, J. S. Chappell, A.N. Bloch, J. P. Ferraris, D. O. Cowan and T. J. Kistenmacher, Mol. Cryst. Liq. Cryst. **87**, 137-161 (1982)
13. A. Morherr, S. Witt, A. Chernenkaya, J.-P. Bäcker, G. Schönhense, M. Bolte, C. Krellner, Physica B **496**, 98-105 (2016)
14. M. Meneghetti , A. Girlando, and C. Pecile, J. Chem. Phys. **83**, 3134 -3145 (1985)
15. P. Hu, K. Du, F. Wei, H. Jiang, and C. Klotz, Cryst. Growth Des. **16**, 3019-3027 (2016)
16. J. Lieffrig, O. Jeannin, A. Vacher, D. Lorcy, P. Auban-Senzier, and M. Fourmigué, Acta Cryst. B **70**, 141-148 (2014)
17. A. Painelli and A. Girlando, J. Chem. Phys. **84**, 5655-5671 (1986)
18. V.M. Yartsev and R. Świetlik, Rev. Solid State Sci. **4**, 69-117 (1990)
19. R. Bozio and C. Pecile, in Spectroscopy of Advanced Materials, Ed. J.H. Clark and R.E. Hester, John Vilej & Sons Ltd 1991, pp. 1-85
20. A. Girlando, A. Painelli and C. Pecile, Mol. Cryst. Liq. Cryst. **120**, 17-26 (1985)
21. A. Painelli and A. Girlando, J. Chem. Phys. **87**, 1705-1711 (1987)
22. M. Meneghetti and C. Pecile, Phys. Rev. B **40**, 12187-12195 (1989)
23. M. Meneghetti and C. Pecile, J. Chem. Phys. **105**, 397-407 (1996)
24. T.J. Kistenmacher, T.J. Emge, A.N. Bloch, D.O. Cowan, Acta Cryst. B **38**, 1193 (1982)
25. A. Frąckowiak, I. Olejniczak, R. Świetlik, O. Jeannin, and M. Fourmigué, J. Phys. Chem. C **120**, 23740-23747 (2016)
26. A. Frąckowiak, R. Świetlik, L. Maulana, D. Liu, M. Dressel, O. Jeannin, and M. Fourmigué, J. Phys. Chem. C **124**, 5552-5558 (2020)
27. F. Wooten, Optical Properties of Solids, 1st ed.; Academic Press: New York, USA, 1972
28. The Voigt spectroscopy function is a four-parameter theoretical model of the spectral line including the Gaussian and Lorentzian types of broadening
29. M.J. Frisch, et al., Gaussian 03, Revision B.03, Gaussian, Inc., Pittsburgh, PA, 2003
30. R.Sun, J.Yao , S.Li and R.Gu, *Vib. Spectrosc.* **47,** 38-43 (2008)
31. A.P.Scott and L.Random, *J. Phys. Chem.* **100,** 16502-16513 (1996)

32. A. Frąckowiak, PhD thesis (in Polish), Institute of Molecular Physics PAN 2021 (ISBN: 978-83-956445-7-3)
33. Jacobsen C. S., Torrance J. B., J. Chem. Phys. **78**, 112 (1983)
34. Hasegawa T., Mochida T., Kondo R., Kagoshima S., Iwasa Y., Akutagawa T., Nakamura T., Saito G., Phys. Rev. B **62**, 10059-10066 (2000)
35. T. Murata, G. Saito, K. Nakamura, M. Maesato, T. Hiramatsu, Y. Yoshida, Cryst. Growth Des. **13**, 2778-2792 (2013)
36. J. S. Chappell et al. J. Am. Chem. Soc. **103**, 2442-2443 (1981)
37. S. Matsuzaki, T. Hiejima, M. Sano, Solid State Commun. **82**, 301-304 (1992)
38. K. Tasaki, S. Matsuzaki, V.M. Yartsev, phys. stat. sol. (b) **203**, 265-279 (1997)
39. A. Girlando, R. Bozio, C. Pecile, J.B. Torrance, Phys. Rev. B **26**, 2306 (1982)
40. R. Bozio, I. Zanon, A. Girlando and C. Pecile, J. Chem. Soc. Faraday Trans. II **74**, 235-248 (1978)
41. A. Łapiński, L.Ouahab, T. Imakubo, Vibr. Spectr. **52**, 22 (2010)
42. M. Meneghetti and C. Pecile, J. Chem. Phys. **84**, 4149 (1986)
43. J. L. Musfeldt, K. Kamarás, D. B. Tanner, Phys. Rev. B **45**, 10197 (1992)
44. R. Świetlik, Synth. Metals **74**, 115-122 (1995)